Selective inhibition of JNK located on mitochondria protects against mitochondrial dysfunction and cell death caused by endoplasmic reticulum stress in mice with LPS-induced ALI/ARDS

CONGCONG LI[1], DEBIN MA[1], YAN CHEN[1], WEI LIU[2], FAGUANG JIN[2] and LIYAN BO[1]

[1]Department of Respiratory and Critical Care Medicine, General Hospital of Northern Theater Command, Shenyang, Liaoning 110016; [2]Department of Respiratory and Critical Care Medicine, Tangdu Hospital, Fourth Military Medical University, Xi'an, Shaanxi 710038, P.R. China

Abstract. Few pharmacological interventions are able to improve the mortality rate of acute lung injury and acute respiratory distress syndrome (ALI/ARDS). The aim of this research was to elucidate whether endoplasmic reticulum (ER) stress and c-Jun-N-terminal kinase (JNK)-mitochondria pathways serve important roles in ALI/ARDS and to determine whether the key component Sab is a potential treatment target. The current study investigated the activation of ER stress and the JNK pathway, the content of JNK located on the mitochondria during ER stress and lipopolysaccharide (LPS)-induced ALI/ARDS by western blot analysis. The treatment effects of Tat-Sab$_{KIM1}$, a selective inhibitor of JNK located on mitochondria were explored by multiple methods including histopathological evaluation, lung cell apoptosis tested by TUNEL assay, mitochondrial membrane permeability and survival analysis. The results verified that ER stress was enhanced during LPS-induced ALI/ARDS and could induce activation of the JNK pathway and JNK-mitochondrial localization as well as mitochondrial dysfunction and cell death. Tat-Sab$_{KIM1}$ alleviated LPS injection-induced lung injury and improved mouse survival rates by specifically inhibiting JNK localization to mitochondria and mito-JNK signal activation without affecting cytosolic/nuclear JNK activation. The protective effect of Tat-Sab$_{KIM1}$ against ALI/ARDS was partly caused by inhibition of the excessive activation of mitochondria-mediated apoptosis and autophagy. These results showed the important role of Sab as a treatment target of ALI/ARDS and the potential treatment effect of Tat-Sab$_{KIM1}$. In conclusion, abnormal activation of the JNK-mitochondrial pathway could significantly disrupt the normal physiological function of lung cells, resulting in the occurrence of ALI/ARDS and selective inhibit of JNK located on mitochondria by Tat-Sab$_{KIM1}$ had a protective effect against the mitochondrial dysfunction and cell death caused by endoplasmic reticulum stress in mice with LPS-induced ALI/ARDS.

Introduction

Acute lung injury and acute respiratory distress syndrome (ALI/ARDS) is one of the leading causes of morbidity and mortality in critically ill patients. ALI/ARDS causes ~75,000 deaths every year in the USA alone (1,2). The mortality associated with ALI/ARDS continues to be 25-40% and few pharmacological interventions are able to improve this mortality rate (1,3).

c-Jun-N-terminal kinase (JNK), a member of the mitogen-activated protein kinase (MAPK) family, is a stress-activated protein kinase that is modulated by the MAPK signaling cascade (4). JNK is also known as stress-activated kinase (SAPK) and it is a key factor that regulates the physiological and pathological reactions of the body (5,6). After sensing cellular or extracellular stress, upstream MAP kinases, such as MAPK kinase kinase (MAP3K) and MAPK kinase (MAP2K), can activate JNK by threonine-tyrosine phosphorylation (7,8). Betigeri *et al* (9) showed that JNK can be activated by some stimuli, such as inflammatory cytokines, bacterial endotoxins, osmotic shock, ultraviolet (UV) radiation and hypoxia. JNK activation regulates the cellular response to stress, such as adaptation to stress or programmed cell death, including apoptosis and necrosis (8). These processes are carried out by regulating the phosphorylation and subcellular localization of the substrates and downstream factors of JNK (10). For example, JNK phosphorylates activator protein-1 (AP-1) and

Correspondence to: Dr Congcong Li or Mrs. Liyan Bo, Department of Respiratory and Critical Care Medicine, General Hospital of Northern Theater Command, 83 Wenhua Road, Shenhe, Shenyang, Liaoning 110016, P.R. China
E-mail: licong1988@hotmail.com
E-mail: boliyan@hotmail.com

increases the AP-1-dependent transcription of genes involved in cell proliferation, inflammatory cytokine production and cell death (10). Li *et al* (11) showed that JNK is involved in the occurrence of ALI/ARDS by regulating the apoptosis of lung cells, activating the nuclear factor kappa-B (NF-κB) pathway and disrupting intercellular tight junctions (12).

Endoplasmic reticulum (ER) stress is a disorder of ER protein-folding homeostasis caused by the accumulation of unfolded and misfolded proteins. During the biosynthesis and assembly of proteins, secretory complex and transmembrane proteins enter the ER as unfolded polypeptides and emerge as folded and processed proteins (13). However, unfolding and misfolding occasionally occur and cause an unfolded protein response (UPR) to repair improperly folded proteins or degrade the proteins that cannot be repaired (14). When these mistakes accumulate and exceed the recovery capacity, ER stress occurs. BiP (also known as Grp78) enters the lumen of the ER after dissociating from protein kinase RNA-activated-like ER kinase (PERK) (15), inositol-requiring transmembrane kinase (IRE-1) (16) and activating transcription factor 6 (AFT6) (17). These changes lead to the dimerization and activation of PERK and IRE-1 as well as the activation of ATF6 (15-17). Irreversible ER stress and ER homeostasis disturbance are related to the deterioration of cellular function and even cell death (13). According to previous studies (13,16,18,19), a number of cellular insults may lead to UPR and ER stress, such as infection, hypoxia, reactive oxygen species (ROS), nutrient deprivation and lack of ATP. Previous studies (13,16,18) have suggested that ER stress is critical to various diseases, such as atherosclerosis, diabetes, non-alcoholic fatty liver disease/non-alcohol related steatohepatitis, obesity and cancer.

Mitochondria are the major producers of ATP in mammalian cells and serve critical roles in a variety of events associated with the initiation of apoptosis (20). These roles include receiving stress signals from the cytosol and other organelles, disrupting electron transport and energy generation, altering the cellular oxidation-reduction state, generating excessive levels of ROS, inducing mitochondrial transmembrane potential (ΔΨ) loss and releasing cytochrome c to the cytosol (21). Moreover, mitochondria are involved in the upregulation of proapoptotic proteins and downregulation of antiapoptotic proteins and these functions include interacting with apoptosis protease-activating factor 1, triggering the activation of caspase-9 and leading to subsequent apoptotic processes (20,21). During these actions, some proteins are translated in the cytosol and imported into the mitochondrion. These proteins carry messages and initiate the changes. JNK is one such protein. Activated JNK can interact with Sab, which is expressed on the mitochondrial outer membrane and translocate to the mitochondria (8). The location of JNK on mitochondria can lead to a sequence of events, such as sustained activation of JNK, loss of ΔΨ, overgeneration of ROS and even cell death (22). Sab is composed of an N-terminal SH3 domain binding site in the intermembrane space, one membrane spanning domain and a JNK kinase interaction motif (KIM) on the C-terminus that faces the cytoplasm (23). Sab is the only docking site for JNK on mitochondria. The knockdown of Sab or inhibition of the JNK-Sab interaction using KIM1 peptides can block the translocation of JNK to mitochondria and inhibit JNK-induced sequence events in

mitochondria (24-26). According to a study conducted by Li *et al* (27), the pathological changes in ALI/ARDS are partly associated with the abnormal regulation of mitochondria and maintaining the stability of mitochondrial function is vital to ameliorating ALI/ARDS as mitochondria serve crucial roles in energy generation, ROS production and cell survival, autophagy and apoptosis modulation.

ER stress can activate JNK through the IRE1α pathway. Studies (28,29) have also confirmed that JNK activation induced by ER stress can also interact with Sab and then lead to the disruption of mitochondrial homeostasis and function. Tunicamycin or brefeldin A (BFA), specific inducers of ER stress, can induce cell apoptosis by triggering ER-induced sustained JNK activation and subsequent JNK-mitochondria localization and silencing of Sab can reverse BFA-induced sustained JNK activation (28).

Accumulating evidence suggests that ER stress and JNK mitochondrial localization serve important roles in mitochondrial dysfunction and cell death and the key component Sab might be a potentially attractive target for ALI/ARDS treatment. However, abnormalities in ER stress and the localization of JNK to the mitochondria are rarely reported with respect to the occurrence and progression of ALI/ARDS and their underlying role in ALI/ARDS remains unknown and requires further study. Therefore, the present study hypothesized that abnormal activation of the JNK-mitochondrial pathway could significantly disrupt the normal physiological function of lung cells, resulting in the occurrence of ALI/ARDS and also suggested that selective inhibition of JNK mitochondrial localization by Tat-Sab$_{KIM1}$ had a protective effect against the mitochondrial dysfunction and cell death caused by ER stress in mice with lipopolysaccharide (LPS)-induced ALI/ARDS.

Materials and methods

Reagents. Antibodies against Bip, p-PERK, PERK, p-IRE1, IRE1, ATF6, Chop and Caspase-3 were obtained from Cell Signaling Technology, Inc. Antibodies against cytochrome c, cytochrome c oxidase IV (COX IV) and GAPDH were purchased from Abcam. Phosphorylated (p)-Bcl-2 (Ser70) rabbit mAb, p-JNK (Thr183/Tyr185) rabbit mAb and JNK rabbit mAb were obtained from Cell Signaling Technology, Inc. LC3 rabbit mAb was purchased from Santa Cruz Biotechnology, Inc. The MDA Assay kit (TBA method) and Hydrogen Peroxide Assay kit were obtained from Nanjing Jiancheng Bioengineering Institute. An *In Situ* Cell Death Detection kit was obtained from Roche Applied Science. Dexamethasone (DEX) was purchased from MilliporeSigma. Tat-scramble (LPSVFGDVGAPSRLPEVSLSPPRRRQR RKKRG-NH2) and Tat-Sab$_{KIM1}$ (GFESLSVPSPLDLSG PRVVAPPRRRQRRKKRG-NH2) were purchased from NeoPeptide. TRIzol was purchased from Thermo Fisher Scientific, Inc.

Animal procedures. The animal procedures conducted in the present study were approved by the Animal Care and Use Committee of the Fourth Military Medical University (approval no. TDLL20160194) and were carried out in accordance with the National Institutes of Health Guide for Care and Use of Laboratory Animals (30). A total of 90 male BALB/c

mice (8 weeks old and weighing 20-24 g) were purchased from the Animal Center of the Fourth Military Medical University and maintained on a 12-h light/dark cycle with free access to food and water; the ambient temperature was 18-26˚C and the relative humidity was 40-70%. The BALB/c mice were randomly divided into the following experimental groups (n=15): the control group, LPS 12 h group (LPS-induced ALI/ARDS was established by intraperitoneal injection of 5 mg/kg LPS), LPS 24 h group, DEX pretreatment group (in which the mice were pretreated intraperitoneally with 2.5 mg/kg body weight DEX 30 min before modelling), Tat-Sab$_{KIM1}$ pretreatment group (in which the mice were pretreated with tracheal injection of 2 mg/kg body weight Tat-Sab$_{KIM1}$ 30 min before modelling) and SP600125 pretreatment group (in which the mice were pretreated with intravenous injection of 20 mg/kg body weight SP600125 30 min before modelling). At the preset time (24 h if not otherwise specified), the mice were euthanized by pentobarbital overdose (200 mg/kg, intraperitoneal injection), the lungs were harvested and samples were collected.

Lung wet (W)/dry (D) weight ratio. To evaluate the severity of pulmonary oedema, the W/D ratio of the lung tissue was calculated. Briefly, the left lungs of the mice were harvested and weighed to determine the wet weight. Then, the lungs were placed in an oven and incubated at 75˚C for 72 h to obtain a constant weight, which was denoted as the dry weight. The W/D ratio was calculated by dividing the wet weight by the dry weight.

Assessment of lung cell apoptosis. To quantify cell apoptosis in the injured mouse lungs, a TUNEL assay was conducted using the *In-Situ* Cell Death Detection kit according to the protocol provided by the manufacturer. Lung tissues were fixed with 4% paraformaldehyde for 24 h at room temperature. Then the lung tissues were paraffin embedded and sectioned at 5 μm). After dewaxing, TUNEL working solution was added to the tissue sections for 1 h at 37˚C to label apoptotic cells, which were then stained with the nuclear stain DAPI (5 μg/ml; Merck KGaA) for 5 min at room temperature. The slides were mounted with 50% glycerol (Merck KGaA). The result was analyzed by a digital imaging system (Pannoramic Viewer 1.15.3; Silicon Graphic, Inc.). Images from three slides/groups were randomly captured and the cells exhibiting positive staining for apoptosis were counted manually.

Histopathological evaluation. Histopathological evaluation was conducted by staining the lung tissue with hematoxylin and eosin (H&E). First, the lung tissue of the mice was harvested at the preset time, fixed with 4% paraformaldehyde at room temperature for 24 h, embedded in paraffin and cut into 5-μm sections before staining with H&E (at room temperature for 3 min). The differences among the groups were examined by optical microscopy.

XBP1 mRNA splicing. XBP1 mRNA splicing was detected by reverse transcription PCR. The tissue samples were homogenized using TRIzol and mRNA was collected. Then, reverse transcription was conducted using the PrimeScript RT reagent kit (Takara Bio, Inc.). The primers used to detect XBP1 (spliced form) and XBP1 mRNA were 5'-GAACCA GGAGTTAAGAACACG-3' (forward) and 5'-AGGCAACAG TGTCAGAGTCC-3' (reverse). Finally, the PCR products were analyzed by agarose gel electrophoresis. The DNA ladder we used was purchased from Beyotime Institute of Biotechnology (cat. no. D0107) and the EtBr was purchased from MilliporeSigma.

Neutrophil numbers in bronchoalveolar lavage fluid (BALF). At the preset time, the mice were euthanized and the lungs were surgically removed. Then, the lungs were lavaged with 1 ml ice-cold PBS three times. Then, the cells in the BALF were harvested by centrifugation (2,500 x g at 4˚C for 5 min). The number of neutrophils was calculated after staining with Wright's stain (at room temperature for 3 min) according to the manufacturer's instructions and pale purple neutrophils were counted using a cell counting plate.

Evans blue extravasation assessment. Evans blue extravasation analysis was used to measure the barrier permeability of the lungs. Evans blue dye (MilliporeSigma; 20 mg/kg) was injected into the mice through the tail vein 30 min before the mice were euthanized and the lungs were surgically removed. Then, Evans blue dye was extracted from the lung tissue by incubation in formamide (3 ml/100 mg) at room temperature for 24 h. Finally, the total Evans blue (μg/g) in each sample was calculated using spectrophotometry (620 nm).

Survival analysis. To observe the mortality rates, the mice were administered LPS (50 mg/kg) intraperitoneally 30 min after pretreatment with DEX (DEX pretreatment group) or Tat-Sab$_{KIM1}$ (Tat-Sab$_{KIM1}$ pretreatment group). Then, the mortality of the mice in each group was recorded every 6 h for 3 days.

Cell culture and treatment. As blood-air barrier disruption is the vital pathophysiological changes during ALI/ARDS and alveolar epithelial cell and vascular endothelium are the important element of alveolar-capillary membrane. So immortalized human umbilical vein endothelial cells (HUVECs) and A549 cells were used to represent endothelial cells and epithelial cells respectively in this study. HUVECs and A549 cells were purchased from Jenniobio Biotechnology Co. HUVECs were cultured in F-12K medium (0.1 mg/ml heparin and 0.03 mg/ml endothelial cell growth supplement; Gibco; Thermo Fisher Scientific, Inc.) with 10% fetal bovine serum (Cytiva) at 37˚C and in a 5% CO_2 atmosphere and A549 cells were cultured in RPMI 1640 medium with 10% fetal bovine serum at 37˚C and in a 5% CO_2 atmosphere. LPS challenge was performed by exposing HUVECs to 1 μg/ml LPS at 37˚C for 12 h before harvesting or testing.

Preparation of mitochondrial and cytosolic/nuclear proteins. Mitochondrial and cytosolic/nuclear proteins were prepared by isolating mitochondria from cells or tissue as described by Xu *et al* (22). Briefly, the mouse lungs were washed and homogenized using isolation buffer (210 mM mannitol, 70 mM sucrose, 5 mM HEPES, 1 mM EGTA and 0.5 mg/ml BSA, pH=7.4). Next, the homogenate was centrifuged at 1,000 x g for 10 min at 4˚C and the supernatant was collected and centrifuged at 10,000 x g for 10 min at 4˚C. This second

supernatant was used as the soluble cytosolic/nuclear fraction with excluded mitochondria and the sedimentation pellet was resuspended in lysis buffer for western blot analysis of the mitochondrial proteins. COX IV was used as an internal mitochondrial control and GAPDH served as the control for other organelles.

Western blot analysis. Protein was extracted by RIPA lysis buffer with protease inhibitor cocktail and the protein concentration was determined by a BCA kit (Beyotime Institute of Biotechnology) according to the protocol provided by the manufacturer. Subsequently, equivalent amounts of proteins (20 μg) were separated by 12% SDS-PAGE and transferred to nitrocellulose membranes. Then, the membranes were blocked with 10% nonfat dry milk in Tris-buffered saline (TBS) at room temperature for 30 min and probed overnight with primary antibodies at 4°C. Subsequently, the membranes were washed with TBST and then incubated with an appropriate horseradish peroxidase-conjugated secondary antibody (1:10,000; cat. no. ab6721; Abcam) at room temperature for 2 h. The immunoreactive target proteins were detected by an enhanced chemiluminescent detection system (Thermo Fisher Scientific, Inc.). Band intensities were quantified using Image Lab 4.1 (Bio-Rad Laboratories, Inc.). The following primary antibodies were used: anti-cytochrome c (1:10,000, cat. no. ab133504, Abcam), anti-p-JNK (1:1,000, cat. no. 4668, Cell Signaling Technology, Inc.), anti-GAPDH (1:2500, cat. no. ab181602, Abcam), anti-JNK (1:1,000, cat. no. 9258, Cell Signaling Technology, Inc.), anti-COX IV (1:1,000, cat. no. ab202554, Abcam), anti-LC3 (1:1,000, cat. no. sc-398822, Santa Cruz Biotechnology, Inc.), anti-phospho-Bcl-2 (Ser70) rabbit mAb (1:1,000, cat. no. 2827, Cell Signaling Technology, Inc.) and anti-cleaved caspase-3 (1:1,000, cat. no. 9664, Cell Signaling Technology, Inc.).

Determination of cell apoptosis. Cell apoptosis was detected by double labelling with annexin-V-FITC (Molecular Probes; Thermo Fisher Scientific, Inc.) and PI (Molecular Probes; Thermo Fisher Scientific, Inc.). Briefly, cells from different groups were harvested with trypsin and washed with PBS. Annexin V-FITC and PI were added to the cells as the manual described (15 min at room temperature in the dark). After labelling, the cell apoptosis ratios were detected and analyzed with flow cytometer (FACScan; BD Biosciences) and the software supplied with the machine. The percentage of early and late apoptotic cells were calculated.

Mitochondrial homeostasis. As the mito-JNK pathway participates in LPS-induced ALI/ARDS, the changes in ROS production and mitochondrial functions following LPS exposure were explored. Briefly, to detect the changes in superoxide anion content, the cells from different groups were stained with dihydroethidium (10 μM) and cultured at 37°C for 30 min to load the fluorescent indicator. Then, the medium was replaced and the fluorescence intensity, which reflected the superoxide anion concentration, was recorded by fluorescence microscopy.

Mitochondrial membrane permeability ($\Delta\Psi$) was also measured using a JC-1 fluorescence ratio of 590:538 nm. Briefly, to detect changes in mitochondrial membrane permeability, the cells from the different groups were stained with JC-1 (10 μM) and cultured at 37°C for 20 min to allow the fluorescent indicator to enter the cells. Then, the medium was replaced. The fluorescence intensity (590 and 538 nm) was recorded by fluorescence microscopy and a fluorescence ratio of 590:538 nm reflected $\Delta\Psi$.

Statistical analysis. Statistical analyses were conducted using GraphPad Prism v8 software (GraphPad Software, Inc.). The data are reported as the mean ± standard error of the mean. Comparisons between experimental groups were performed by one-way ANOVA and the Bonferroni test. $P < 0.05$ was considered to indicate a statistically significant difference.

Results

ER stress is enhanced during LPS-induced ALI/ARDS. To characterize the role and status of ER stress in LPS-induced ALI/ARDS, the expression of the ER stress sensors Bip/GRP78 and ATF6 and the phosphorylation of PERK and IRE-1 were determined by western blotting. The data (as shown in Fig. 1A) showed that the expression of both Bip and ATF6 was significantly increased after LPS challenge compared with those in the control group and this was especially true in the LPS 24 h group; these results indicated the activation of ER stress. In contrast, the expression of these proteins in the DEX pretreatment group was decreased compared with that in the LPS 24 h group. In addition, LPS also increased the phosphorylation of PERK, which was slightly but significantly attenuated by DEX pretreatment (Fig. 1A). A similar change was also detected in IRE-1 (Fig. 1A). The results suggested that anti-inflammatory therapy with dexamethasone could alleviate LPS-induced ER stress during ALI/ARDS.

To further confirm the occurrence of ER stress, the splicing of XBP-1 was also detected; this is the active form of the transcription factor XBP-1. XBP-1 is one of the downstream signaling molecules of IRE-1 and it can increase protein folding, reduce protein translation and eventually restore protein folding homeostasis. As shown in Fig. 1B, the amount of spliced XBP-1 was elevated in the lung after intraperitoneal LPS injection. Collectively, these results clearly indicated that ER stress in the lung was enhanced during LPS-induced ALI/ARDS.

ER stress can induce mitochondrial dysfunction and cell death in A549 cells and HUVECs. Next, the effect of ER stress pathway activation on lung cells, which were represented by A549 cells and HUVECs was explored. First the expression of apoptosis-related genes, such as p-Bcl-2, cleaved caspase-3 and Bax and the leakage of cytochrome c into the cytosol were detected (Fig. 2A). After treatment with the ER stress activator tunicamycin (20 μg/ml), more cytochrome c was released from mitochondria to the cytosol in both A549 cells and HUVECs and less p-Bcl-2 and more cleaved caspase-3 and Bax were detected in the activated groups. These results indicated that ER stress activated by tunicamycin could lead to the excessive activation of apoptosis pathways.

The leakage of cytochrome c indicated that an oxidant-antioxidant imbalance might occur. For confirmation, the changes in ROS production and mitochondrial function upon
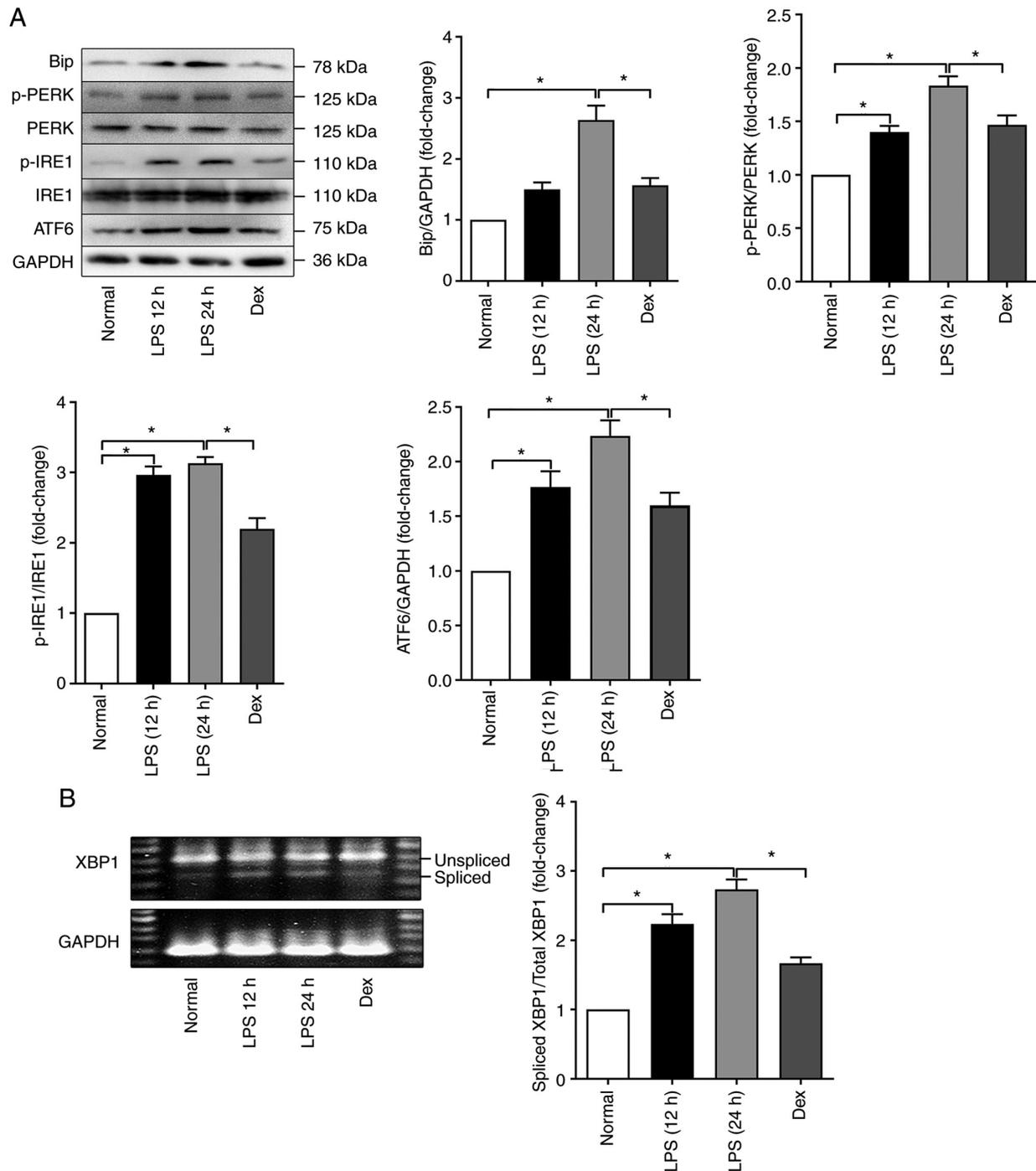
Figure 1. LPS treatment induces ER stress in the lungs of mice. (A) Representative western blots of ER stress-related genes (Bip, p-PERK, PERK, p-IRE1, IRE1 and ATF6) in the Normal, LPS 12 h, LPS 24 h and Dex groups. (B) Splicing of XBP-1 in the Normal, LPS 12 h, LPS 24 h and Dex groups. The data are expressed as the mean ± standard error of the mean, n=4/group, *P<0.05. LPS, lipopolysaccharide; ER, endoplasmic reticulum; p-, phosphorylated; PERK, protein kinase RNA-activated-like ER kinase; IRE1, inositol-requiring transmembrane kinase; ATF6, activating transcription factor 6.

ER stress were further explored. The results (as shown in Fig. 2B) showed that tunicamycin exposure could significantly elevate the production of ROS in both A549 cells and HUVECs. The mitochondrial membrane permeability ($\Delta\Psi$) and $\Delta\Psi$ dissipation was detected using a JC-1 fluorescence ratio of 590:538 nm. These results suggest that overactivation of ER stress could induce mitochondrial dysfunction and ROS accumulation and even lead to apoptosis.

Cell apoptosis were quantitated by flow cytometry with annexin-V-FITC and PI double labelling. The results (Fig. 2C) showed that tunicamycin increased the percentage of apoptotic cells to >20%. All of these results indicated that ER stress could induce mitochondrial dysfunction and cell death in A549 cells and HUVECs.

ER stress can induce activation of JNK and JNK mitochondrial localization in A549 cells and HUVECs. To elucidate the role of JNK, especially the mitochondria-JNK interaction, during ER stress, the expression of p-JNK and JNK was assessed in total cellular proteins, mitochondrial proteins
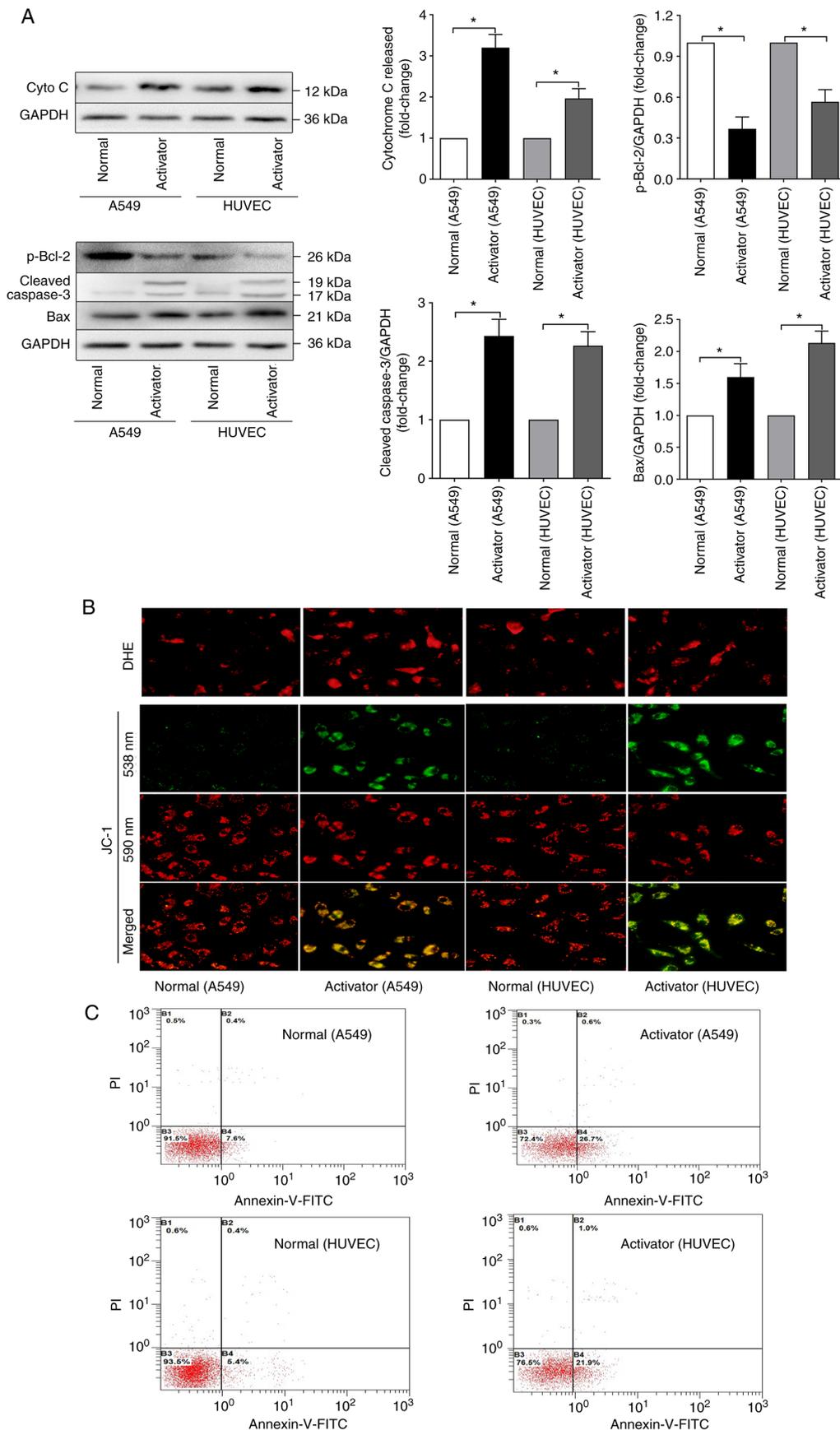
Figure 2. ER stress can induce mitochondrial dysfunction and cell death. (A) Representative western blots of cyto c leakage to the cytosol, p-Bcl-2, cleaved caspase3 and Bax in HUVECs and A549 cells treated with the ER stress activator tunicamycin. (B) Changes in superoxide anion content and mitochondrial membrane permeability (ΔΨ) after HUVECs and A549 cells were treated with the ER stress activator tunicamycin; magnification, x200. (C) Cell apoptosis detected by double labelling of HUVECs and A549 cells treated with the ER stress activator tunicamycin with annexin-V-FITC and PI. The data are expressed as the mean ± standard error of the mean, n=4/group, *P<0.05. ER, endoplasmic reticulum; cyto c, cytochrome c; HUVECs, human umbilical vein endothelial cells; p-, phosphorylated; DHE, dihydroethidium.
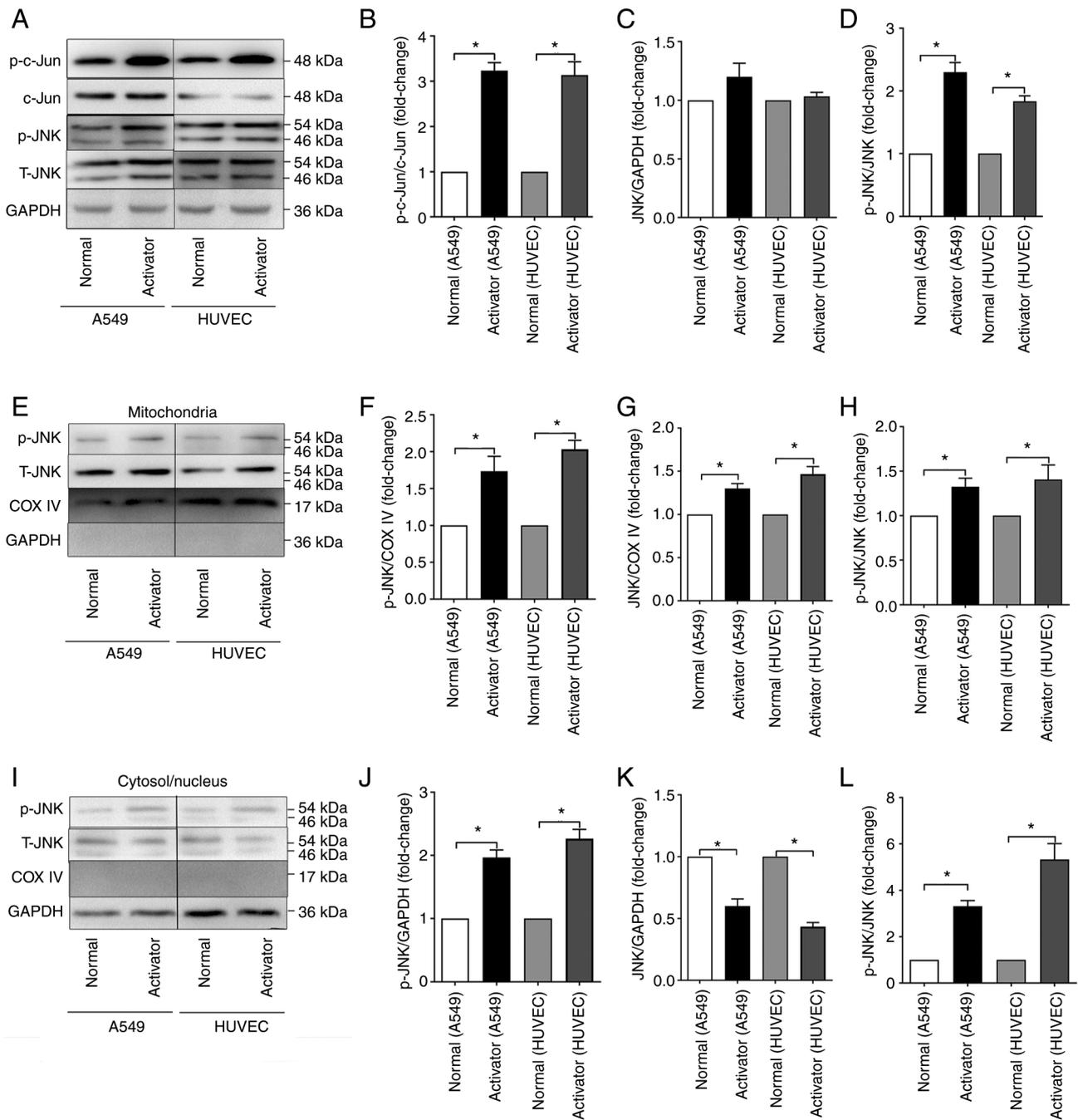
Figure 3. ER stress can induce activation of JNK and mitochondrial localization of JNK in A549 cells and HUVECs. (A) Representative western blots of p-c-Jun, c-Jun, p-JNK and JNK in the total proteins of HUVECs and A549 cells treated with the ER stress activator tunicamycin. (B) Normalized ratio of p-c-Jun/c-Jun in the total proteins. (C) Relative content of JNK in the total proteins. (D) Normalized ratio of p-JNK/JNK in the total proteins. (E) Representative western blots of p-JNK and JNK in the mitochondrial proteins. (F) Relative content of p-JNK in the mitochondrial proteins. (G) Relative content of JNK in the mitochondrial proteins. (H) Normalized ratio of p-JNK/JNK in the mitochondrial proteins. (I) Representative western blots of p-JNK and JNK in the cytosolic/nuclear proteins. (J) Relative content of p-JNK in the cytosolic/nuclear proteins. (K) Relative content of JNK in the cytosolic/nuclear proteins. (L) Normalized ratio of p-JNK/JNK in the cytosolic/nuclear proteins. The data are expressed as the mean ± standard error of the mean. n=4/group. $^*P<0.05$. ER, endoplasmic reticulum; HUVECs, human umbilical vein endothelial cells; p-, phosphorylated; t-, total; COX IV, cytochrome c oxidase IV.

and cytosolic/nuclear proteins by western blotting. According to the results (Fig. 3), ER stress induced by tunicamycin could activate the JNK pathway by phosphorylating JNK and c-jun. Furthermore, it was found that the phosphorylation level of JNK was significantly elevated in both the mitochondria and cytosol/nucleus after tunicamycin challenge. Although the total JNK in the mitochondria was also elevated, that in the cytosol/nucleus was decreased, indicating that ER stress

could induce JNK translocation from the cytosol/nucleus to mitochondria in A549 cells and HUVECs.

LPS induces JNK activation and JNK mitochondrial localization in mice. To further observe the role of the mitochondria-JNK interaction in LPS-induced ALI/ARDS, the activation of JNK pathways in the lungs was detected following LPS challenge. According to the results (Fig. 4), p-JNK and
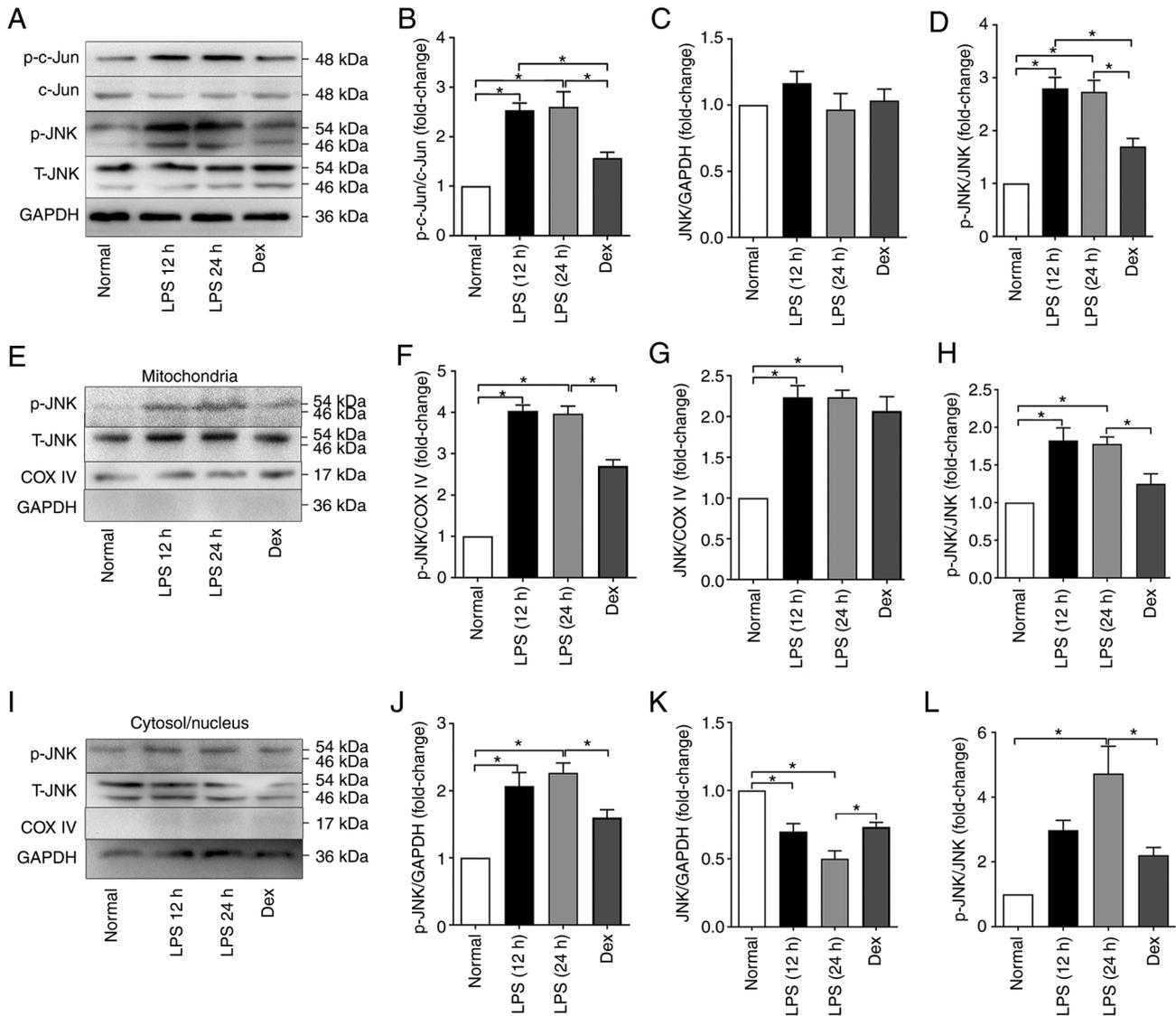
Figure 4. LPS induced JNK activation and JNK mitochondrial localization in mice. (A) Representative western blots of p-c-Jun, c-Jun, p-JNK and JNK in the total proteins of the Normal, LPS 12 h, LPS 24 h and Dex groups. (B) Normalized ratio of p-c-Jun/c-Jun in the total proteins. (C) Relative content of JNK in the total proteins. (D) Normalized ratio of p-JNK/JNK in the total proteins. (E) Representative western blots of p-JNK and JNK in the mitochondrial proteins. (F) Relative content of p-JNK in the mitochondrial proteins. (G) Relative content of JNK in the mitochondrial proteins. (H) Normalized ratio of p-JNK/JNK in the mitochondrial proteins. (I) Representative western blots of p-JNK and JNK in the cytosolic/nuclear proteins. (J) Relative content of p-JNK in the cytosolic/nuclear proteins. (K) Relative content of JNK in the cytosolic/nuclear proteins. (L) Normalized ratio of p-JNK/JNK in the cytosolic/nuclear proteins. The data are expressed as the mean ± standard error of the mean, n=4/group, *P<0.05. LPS, lipopolysaccharide; p-, phosphorylated; t-, total; Dex, dexamethasone; COX IV, cytochrome c oxidase IV.

c-jun in the lung tissues were elevated following intraperitoneal LPS injection, especially in the 24 h group. The amount of JNK mitochondrial localization during LPS-induced ALI/ARDS was also detected by western blotting. Similar to tunicamycin exposure, LPS exposure could induce the phosphorylation of JNK in both mitochondria and the cytosol/nucleus. The total JNK in the mitochondria was also elevated in the LPS groups, whereas that in the cytosol/nucleus was decreased, indicating that in LPS-induced ALI/ARDS, JNK could translocate from the cytosol/nucleus to mitochondria.

The protective role of DEX was also examined. As shown in Fig. 4, DEX pretreatment significantly alleviated the LPS-induced increase in phosphorylated JNK in both the mitochondria and cytosol/nucleus, whereas it did not affect the total JNK content.

Efficiency of Tat-Sab$_{KIM1}$ and SP600125 on JNK activation. To further explore the effect of JNK mitochondrial localization during LPS-induced ALI/ARDS, the protective effects of SP600125 and Tat-Sab$_{KIM1}$ were first verified. SP600125 is a specific inhibitor of the JNK pathway. Tat-Sab$_{KIM1}$ is a peptide that can act on the Sab$_{KIM1}$ domain expressed in mitochondria and selectively block JNK translocation to mitochondria both *in vitro* and *in vivo* by inhibiting the binding of JNK to Sab$_{KIM1}$. Tat-Sab$_{KIM1}$ does not exert any effect on JNK translocation to the nucleus. As shown in Fig. 5, tracheal Tat-Sab$_{KIM1}$ injection significantly decreased the level of phosphorylated JNK and the total JNK level in mitochondria. Tat-Sab$_{KIM1}$ also inhibited the LPS-induced decrease in the total JNK level in the cytosol/nucleus. These results indicated that Tat-Sab$_{KIM1}$ could specifically
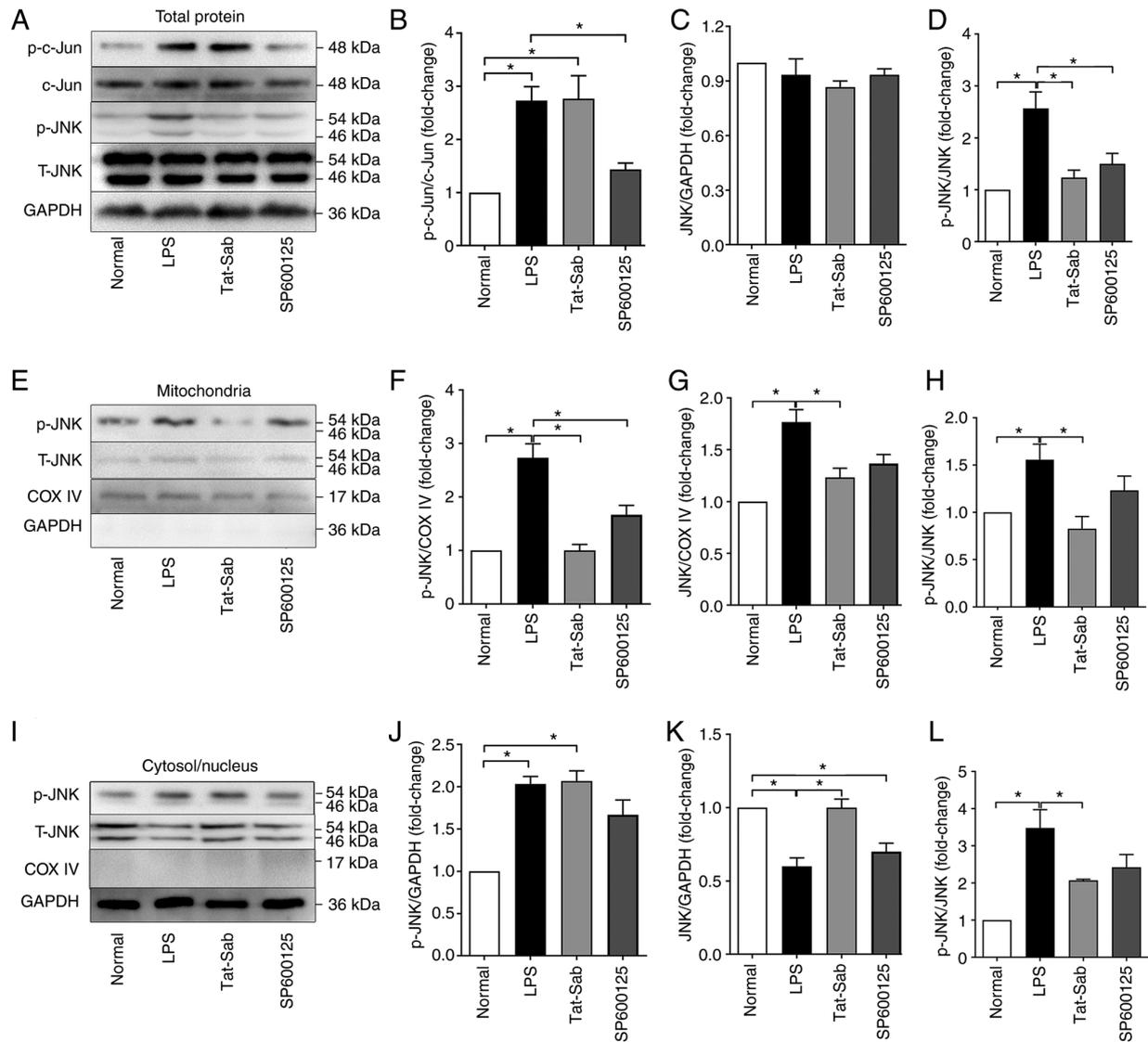
Figure 5. Efficiency of Tat-Sab$_{KIM1}$ and SP600125 on the activation of JNK. (A) Representative western blots of p-c-Jun, c-Jun, p-JNK and JNK in the total proteins of the Normal, LPS, Tat-Sab$_{KIM1}$ and SP600125 groups. (B) Normalized ratio of p-c-Jun/c-Jun in the total proteins. (C) Relative content of JNK in the total proteins. (D) Normalized ratio of p-JNK/JNK in the total proteins. (E) Representative western blots of p-JNK and JNK in the mitochondrial proteins. (F) Relative content of p-JNK in the mitochondrial proteins. (G) Relative content of JNK in the mitochondrial proteins. (H) Normalized ratio of p-JNK/JNK in the mitochondrial proteins. (I) Representative western blots of p-JNK and JNK in the cytosolic/nuclear proteins. (J) Relative content of p-JNK in the cytosolic/nuclear proteins. (K) Relative content of JNK in the cytosolic/nuclear proteins. (L) Normalized ratio of p-JNK/JNK in the cytosolic/nuclear proteins. The data are expressed as the mean ± standard error of the mean, n=4/group, *P<0.05. KIM, kinase interaction motif; p-, phosphorylated; t-, total; COX IV, cytochrome c oxidase IV.

inhibit JNK localization to mitochondria and mito-JNK signal activation without affecting cytosolic/nuclear JNK activation. SP600125 also inhibited the phosphorylation of c-jun and JNK. However, it had no selective effect on the distribution of JNK.

Treatment effect of Tat-Sab$_{KIM1}$ on LPS-induced ALI/ARDS. As Tat-Sab$_{KIM1}$ can selectively inhibit JNK mitochondrial localization, it was further utilized to explore the role of mitochondrial JNK pathway activation in the progression of ALI/ARDS. As shown in Fig. 6A, the mice in the control group had clear and normal alveolar structures. Tat-Sab$_{KIM1}$ allevi-ated LPS injection-induced lung tissue structure destruction, alveolar wall thickening, interstitial lung inflammatory cells and liquid exudation.

To observe pulmonary oedema, the W/D rate was also measured (Fig. 6B). LPS caused pulmonary oedema and the W/D ratio of the LPS group was nearly twice that of the control group. Pretreatment with Tat-Sab$_{KIM1}$ significantly alleviated tissue oedema.

In addition, the cell number in the BALF and Evans blue extravasation were measured to evaluate the barrier perme-ability of the lungs. The results (Fig. 6C and D) suggested that Tat-Sab$_{KIM1}$ could maintain the barrier function of the lung and exert a protective effect against ALI/ARDS.

These results were consistent with those of the survival analysis (Fig. 6E). The number of deaths 72 h after LPS in the LPS group was significantly higher than that in the control groups. Tat-Sab$_{KIM1}$ treatment significantly improved the mouse survival rates compared with LPS treatment alone.
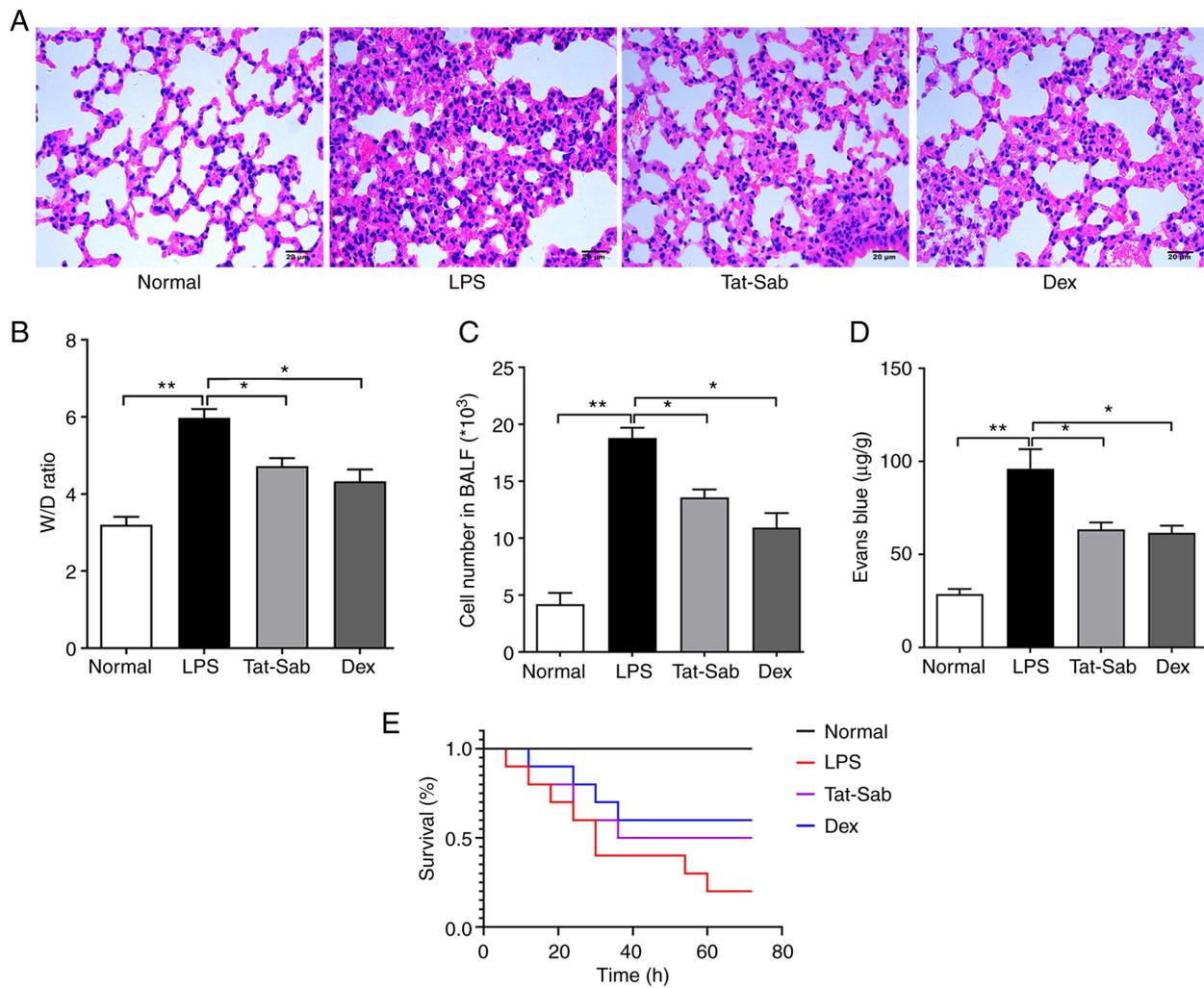
Figure 6. Treatment effect of Tat-Sab$_{KIM1}$ on LPS-induced ALI/ARDS. (A) Histological changes in mouse lung tissue of the Normal, LPS, Tat-Sab$_{KIM1}$ and Dex groups; magnification, x200. (B) Change in the lung W/D ratio of the Normal, LPS, Tat-Sab$_{KIM1}$ and Dex groups. (C) Cell number in BALF of the Normal, LPS, Tat-Sab$_{KIM1}$ and Dex groups. (D) Evans blue extravasation assessment of the Normal, LPS, Tat-Sab$_{KIM1}$ and Dex groups. The data are expressed as the mean ± standard error of the mean, n=4/group, *P<0.05, **P<0.01. (E) Survival analysis of the Normal, LPS, Tat-Sab$_{KIM1}$ and Dex groups. n=10/group, *P<0.05. LPS, lipopolysaccharide; ALI/ARDS, acute lung injury and acute respiratory distress syndrome; p-, phosphorylated; t-, total; Dex, dexamethasone; W/D, wet/dry; BALF.

Effect of Tat-Sab$_{KIM1}$ on cell death in the mouse lung. Apoptosis was also examined during LPS-induced ALI/ARDS and the protective effect of Tat-Sab$_{KIM1}$. As shown in Fig. 7A, in the LPS group, the release of cytochrome c from the mitochondria into the cytosol was considerably increased compared to that in the control group. Treatment with Tat-Sab$_{KIM1}$ or DEX reduced cytochrome c release from the mitochondria. The expression of p-Bcl-2, cleaved caspase-3 and Bax was also detected. More p-Bcl-2 and less cleaved caspase-3 and Bax were detected in the Tat-Sab$_{KIM1}$ groups than in the LPS group. These results indicated that blocking JNK mitochondrial localization could inhibit the excessive activation of apoptosis pathways.

The cell apoptosis ratio in the lungs by was also detected TUNEL staining. The results (Fig. 7B) indicated that the inhibition of mitochondrial JNK signaling exerted an anti-apoptotic effect. Tat-Sab$_{KIM1}$ treatment significantly decreased the number of TUNEL-positive cells compared with LPS treatment alone. These results indicated that mitochondrial JNK signaling participated in mitochondria-mediated apoptosis during ALI/ARDS.

Effect of Tat-Sab$_{KIM1}$ on mitochondrial function in HUVECs. The results from Xu *et al* (22) indicate that JNK mitochondrial localization might disrupt the function of mitochondria and even lead to cell death. To confirm the disruption of mitochondrial functions, the present study explored the changes in cytochrome c leakage, ROS production and ΔΨ in HUVECs during LPS challenge. As epithelial cells, A549 cells cannot be affected and injured by LPS directly. LPS is generate by G-bacteria and released into blood and the endothelial cells rather than epithelial cells can contact with LPS directly. Thus, LPS was used to intervene HUVECs in the *in vitro* experiments. The results (Fig. 8) showed that LPS exposure could significantly elevate the leakage of cytochrome c in HUVECs and Tat-Sab$_{KIM1}$ could eliminate this. The changes in ROS production and ΔΨ dissipation induced by LPS could also be alleviated by Tat-Sab$_{KIM1}$. These results suggested that LPS could induce mitochondrial dysfunction and ROS accumulation and these changes could be alleviated when JNK mitochondrial localization was blocked by Tat-Sab$_{KIM1}$.
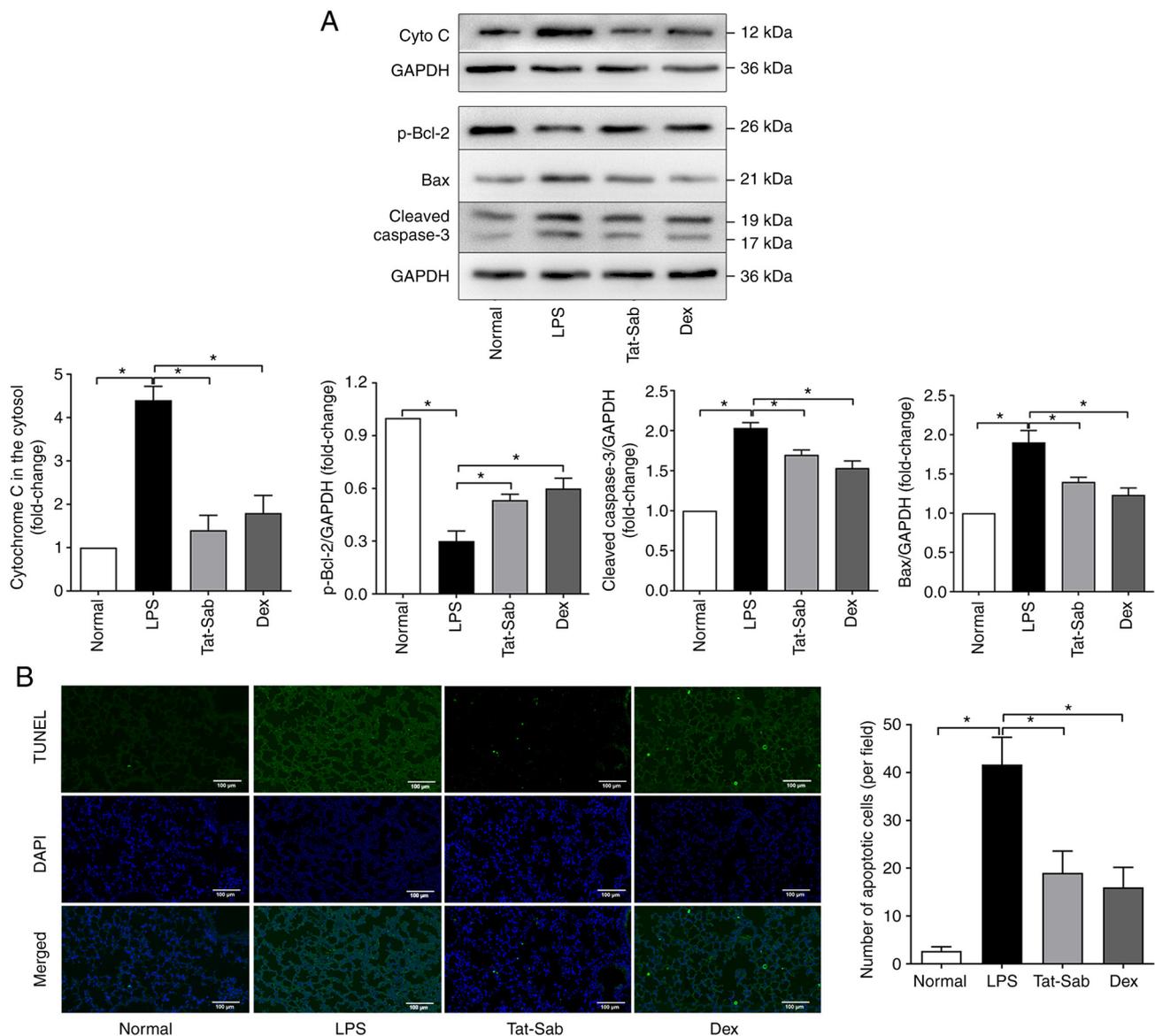
Figure 7. Effect of Tat-Sab$_{KIM1}$ on cell death in the mouse lung. (A) Representative western blots of cyto c in the cytosol, p-Bcl-2, cleaved caspase3 and Bax of the Normal, LPS, Tat-Sab$_{KIM1}$ and Dex groups. (B) Changes in the cell apoptosis ratio in the lungs detected by TUNEL staining of the Normal, LPS, Tat-Sab$_{KIM1}$ and Dex groups; magnification, x100. The data are expressed as the mean ± standard error of the mean, n=4/group, $^*P<0.05$. cyto c, cytochrome c; p-, phosphorylated; t-, total; Dex, dexamethasone; LPS, lipopolysaccharide.

Effect of Tat-Sab$_{KIM1}$ on autophagy in the mouse lung. Autophagy has been demonstrated to participate in the development of ALI/ARDS, as per the conversion of LC3, i.e., LC3-I to LC3-II (31). ATG5 might also modulate autophagy. As shown in Fig. 9, LPS exposure increased the conversion of LC3 to LC3-II, which is the active form and increased the expression of ATG5. The inhibition of mitochondrial JNK by Tat-Sab$_{KIM1}$ restored the levels of ATG5 and LC3, indicating that the inhibition blocked the autophagy induced by ALI/ARDS.

Discussion

The mortality rate associated with ALI/ARDS varies between 25-40%. To date, there is no evidence showing that any pharmacological interventions are associated with an ameliorative mortality rate (1,3). ALI/ARDS can be caused by diseases such as pneumonia, trauma and sepsis, which means that the heterogeneity of its etiology is huge. Therefore, it is difficult to elucidate the pathogenesis of ALI/ARDS and identify drugs with definite effects.

The present study mainly explored the role of ER stress and JNK-mitochondria pathways in ALI/ARDS. The major goal was to explore ER stress-JNK-mitochondria abnormalities during ALI/ARDS and confirm the hypothesis that abnormal activation of the JNK-mitochondrial pathway could significantly disrupt the normal physiological function of lung cells, resulting in the occurrence of ALI/ARDS. Furthermore, selective inhibition of JNK mitochondrial localization by Tat-Sab$_{KIM1}$ had a protective effect against mitochondrial dysfunction and cell death caused by ER stress in mice with LPS-induced ALI/ARDS.

Studies have implicated ER stress-related cellular dysfunction and cell death in the occurrence and progression
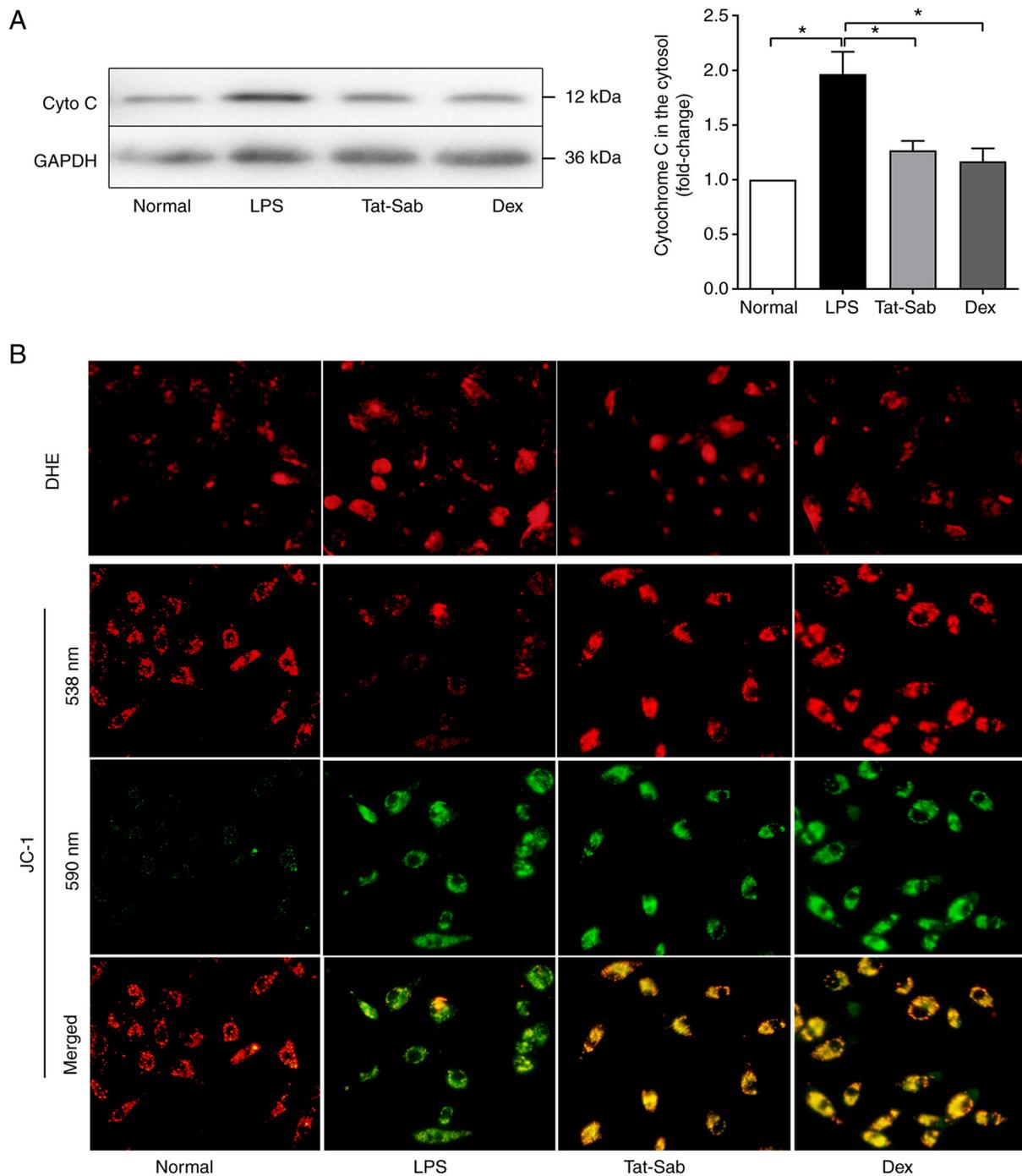
Figure 8. Effect of Tat-Sab$_{KIM1}$ on mitochondrial function in HUVECs. (A) Representative western blots of cyto c in the cytosol of HUVECs. (B) Changes in superoxide anion content and mitochondrial membrane permeability ($\Delta\Psi$) after HUVECs were challenged with LPS and pre-treated with Tat-Sab$_{KIM1}$ or Dex; magnification, x200. The data are expressed as the mean ± standard error of the mean, n=4/group, *P<0.05. HUVECs, human umbilical vein endothelial cells; cyto c, cytochrome c; p-, phosphorylated; t-, total; cyto c, cytochrome c; LPS, lipopolysaccharide; Dex, dexamethasone; DHE, dihydroethidium.

of a number of diseases and these changes may be potential therapeutic targets (13,16,18). Under normal circumstances, BiP/GRP78 binds to the ER stress sensor proteins PERK, IRE1 and ATF6, which prevents their dimerization and UPR activation. However, during the stress response, the accumulation of unfolded proteins leads to the release of BiP/GRP78 from IRE1α, ATF6 and PERK and then to the activation of downstream signaling components, such as XBP-1, eIF2α, ATF4 and cleaved ATF6 (15-17). These reactions are helpful for protein folding and degradation and ER expansion.

After releasing BiP/GRP78, activated PERK dimerizes and phosphorylates eIF2α, which can suppress 5'-capped mRNA translation (14,15). The cleaved ATF6 fragment can modulate apoptosis and protein folding by regulating the expression of some ER chaperones. XBP-1 can lead to ER-associated degradation by upregulating the expression of ER chaperones and genes. XBP-1 activation is initiated by the splicing of XBP-1 mRNA by activated IRE1α and then, the spliced XBP-1 mRNA binds to open reading frames and promotes translation (32).
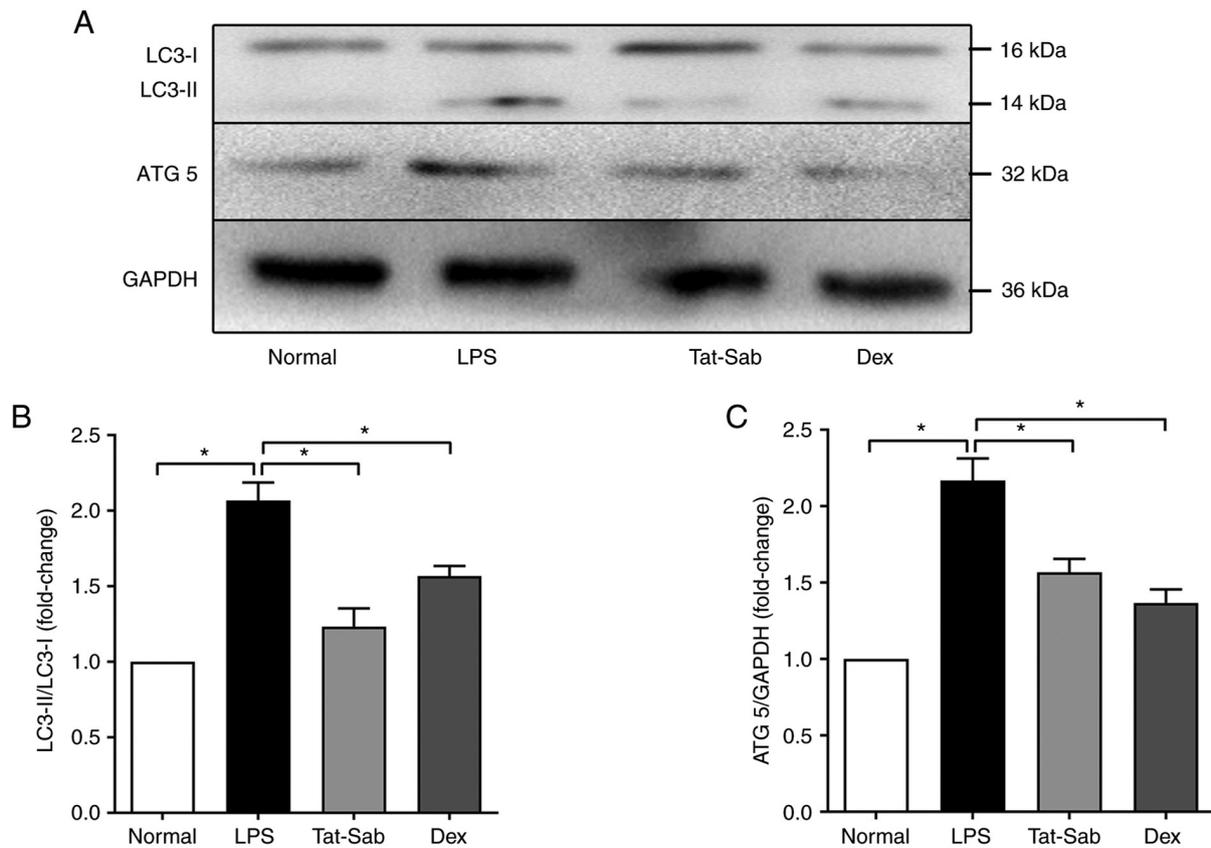
Figure 9. Effect of Tat-Sab_{KIM1} on autophagy in the mouse lung. (A) Representative western blots of LC-3 and ATG5 in the Normal, LPS, Tat-Sab_{KIM1} and Dex groups. (B) Normalized ratio of LC3-II/LC3-I. (C) Relative content of ATG5. The data are expressed as the mean ± standard error of the mean, n=4/group, *P<0.05. LPS, lipopolysaccharide; Dex, dexamethasone

The experimental results of the present study demonstrated that ER stress was enhanced during LPS-induced ALI/ARDS. Bip/GRP78 and p-PERK and ATF6 were significantly increased after LPS challenge, indicating the activation of ER stress. The percentage of spliced XBP-1 was elevated in the lung after intraperitoneal LPS injection.

Li *et al* (33) show that IRE1α can also activate JNK by recruiting TRAF2 and ASK1. JNK regulates cellular adaptation to stress and causes cell death. Vannuvel *et al* (29) show that JNK can translocate to the mitochondrial outer membrane following activation and then lead to Bim phosphorylation and activation. Then, Bim induces the oligomerization of Bax and Bak, finally resulting in the release of cytochrome c and activation of the caspase-dependent apoptotic pathway.

In the present study, tunicamycin, a specific and widely used chemical inducer of lethal ER stress, inhibited protein glycosylation in the ER and led to ER stress due to protein misfolding. ER stress could induce mitochondrial dysfunction and cell death in lung cells, which were represented by A549 cells and HUVECs. Tunicamycin exposure significantly increased ROS production and ΔΨ dissipation. Tunicamycin increased the percentage of apoptotic cells to >20% and more cytochrome c was released from mitochondria into the cytosol. Less p-Bcl-2 and more cleaved caspase-3 and Bax were detected in the activated groups. These results suggested that overactivation of ER stress could induce mitochondrial dysfunction and ROS accumulation and even lead to apoptosis.

Studies (23,25,26,34) show that JNK can transfer from cytoplasm to mitochondria in some conditions by interacting with Sab, which expresses in the outer membrane of mitochondria. Following knockdown of Sab, the change of JNK in cytoplasm and mitochondria is prevented. N-terminal KIM in Sab is essential for JNK binding and confocal immunocytochemistry and cell fractionation studies indicate that Sab is associated with mitochondria, where it co-localizes with a fraction of JNK. These reported properties of Sab suggest its role in targeting JNK to this subcellular compartment (mitochondria). The present study used western blot analysis to detect the transfer of JNK as previous studies (22,35) report and proved that ER stress could induce JNK activation and mitochondrial localization in A549 cells and HUVECs. The total JNK in the mitochondria was also elevated, whereas that in the cytosol/nucleus was decreased, indicating that ER stress could induce JNK translocation from the cytosol/nucleus to mitochondria in A549 cells and HUVECs. Therefore, blocking the interaction of JNK with mitochondria and inhibiting secondary apoptosis might be potential therapeutic targets.

Previous studies (8,22,28) show that JNK can interact with mitochondria by binding to Sab (SH3BP5). Sab is a mitochondrial outer membrane protein with one SH3 domain binding site at the N-terminus, one membrane spanning domain and two D-motifs (KIMs) at the C-terminus. KIM is similar to c-Jun and can link JNK with Sab. Studies (22,26,35) also prove that the activation of JNK and interaction with mitochondria by the docking protein Sab are involved in the regulation of

mitochondrial functions, impairment of electron transport and mitochondrial bioenergetics and participation in ROS generation and apoptosis.

As Sab is the only JNK docking site in mitochondria, depleting Sab could completely prevent JNK translocation to mitochondria. Previous studies (26,36) show that knockdown of Sab blocks JNK translocation to mitochondria in *in vivo* or *in vitro* models of JNK-dependent toxicity (APAP, TNF/GalN, ER stress and palmitic acid lipotoxicity) and inhibit JNK activation-induced mitochondrial dysfunction and cell death. Study (28) showed that silencing Sab in PMH and HeLa cells can prevent BFA-induced JNK-mitochondria pathway activation and subsequent cell death. The synthesis of the KIM1-specific binding peptide Tat-Sab$_{KIM1}$ can also selectively block the binding of JNK to Sab without blocking the kinase activity of JNK, the ratio of p-JNK/JNK or the activation of cytosolic/nuclear JNK (22). The results of the present study showed that Tat-Sab$_{KIM1}$ could successfully reach the cytoplasm through the cell membrane, its concentration was stable and the concentration in the cells after 24 h could still reach the initial concentration of up to 90% (34). Therefore, Tat-Sab$_{KIM1}$ might be optimal for blocking the binding of Sab and JNK. Studies (22,24) have shown that inhibition of p-JNK binding to Sab using Tat-Sab$_{KIM1}$ prevents ischemic necrosis in the heart and brain.

ER stress could trigger the interaction of JNK with mitochondrial Sab, followed by impaired respiration and increased mitochondrial ROS and cell death. ROS accumulation was significantly blocked by Tat-Sab$_{KIM1}$ but not by scrambled peptide. Therefore, it was hypothesized that in ALI/ARDS, abnormal activation of the JNK-mitochondrial pathway could significantly disrupt the normal physiological function of lung cells and the initial activation of JNK in the ER is followed by its interaction with Sab, leading to impaired mitochondrial function and amplification of mitochondrial ROS release and serving a key role in the occurrence of ALI/ARDS. Selective inhibition of the mitochondrial localization of JNK by Tat-Sab$_{KIM1}$ protected against the mitochondrial dysfunction and cell death caused by endoplasmic reticulum stress in LPS-induced ALI/ARDS mice.

The present study verified this hypothesis and showed that LPS induced JNK activation and JNK mitochondrial localization in mice. In LPS-induced ALI/ARDS, LPS exposure induced the phosphorylation of JNK in both mitochondria and the cytosol/nucleus. The total JNK expression in the mitochondria was also increased in the LPS groups, whereas that in the cytosol/nucleus was decreased, indicating that in LPS-induced ALI/ARDS, JNK could translocate from the cytosol/nucleus to mitochondria. Tat-Sab$_{KIM1}$ specifically inhibited JNK localization to mitochondria and the activation of mito-JNK signaling without affecting cytosolic/nuclear JNK activation. Tat-Sab$_{KIM1}$ does not exhibit any effect on the translocation of JNK to the nucleus. The experimental results of the present study also showed that Tat-Sab$_{KIM1}$ could alleviate LPS injection-induced lung tissue structure destruction, alveolar wall thickening, interstitial lung inflammatory cells and liquid exudation. Tat-Sab$_{KIM1}$ treatment significantly improved the mouse survival rates compared with LPS treatment alone. Blocking JNK mitochondrial localization also inhibited the excessive activation of apoptosis pathways.

Tat-Sab$_{KIM1}$ treatment significantly decreased the number of TUNEL-positive cells compared with LPS treatment alone. These results indicated that mitochondrial JNK signaling participated in mitochondria-mediated apoptosis during ALI/ARDS. LPS could induce mitochondrial dysfunction and ROS accumulation and these changes could be alleviated when JNK mitochondrial localization was blocked by Tat-Sab$_{KIM1}$. The inhibition of mitochondrial JNK by Tat-Sab$_{KIM1}$ restored the levels of ATG5 and LC3, indicating that mitochondrial JNK inhibition blocked the autophagy induced by ALI/ARDS. Therefore, inhibiting the translocation of JNK to mitochondria can be used to repair damage by protecting the normal physiological function of organelles.

There are also some limitations in this study that should be mentioned. Alveolar epithelial cells and pulmonary vascular endothelial cells extracted from LPS-interfered animals might be the best choice to explore ALI/ARDS *in vitro*. However, because extracting and cultivate primary cells needed time and the effect of LPS on the extracted cells from LPS-interfered animals might already lose efficacy, so HUVECs and A549 cells were used instead.

Collectively, the results presented clearly indicated that during ALI/ARDS, abnormal activation of ER stress and JNK-mitochondrial pathways could significantly disrupt the normal physiological function of lung cells, resulting in the occurrence of ALI/ARDS. Through selective inhibition, JNK mitochondrial localization by Tat-Sab$_{KIM1}$ exerted a protective effect against the mitochondrial dysfunction and cell death caused by ER stress in mice with LPS-induced ALI/ARDS.

Acknowledgements

Funding

Availability of data and materials

The datasets used and/or analyzed during the current study are available from the corresponding author on reasonable request.

Authors' contributions

CL and LB contributed to the study design. LB, DM and YC also contributed to the conduct of the study. WL and FJ contributed to the data analysis. CL and LB confirm the authenticity of all the raw data. All authors contributed to drafting the manuscript and have read and approved the final manuscript.

Ethics approval and consent to participate

The animal procedures conducted in the present study were approved by the Animal Care and Use Committee of the Fourth Military Medical University (approval no. TDLL20160194)

and were carried out in accordance with the National Institutes of Health Guide for Care and Use of Laboratory Animals (30).

Patient consent for publication

Not applicable.

Competing interests

The authors declare that they have no competing interests.

References

1. ARDS Definition Task Force; Ranieri VM, Rubenfeld GD, Thompson BT, Ferguson ND, Caldwell E, Fan E, Camporota L and Slutsky AS: Acute respiratory distress syndrome: The berlin definition. JAMA 307: 2526-2533, 2012.
2. Rubenfeld GD, Caldwell E, Peabody E, Weaver J, Martin DP, Neff M, Stern EJ and Hudson LD: Incidence and outcomes of acute lung injury. N Engl J Med 353: 1685-1693, 2005.
3. Fan E, Brodie D and Slutsky AS: Acute respiratory distress syndrome: Advances in diagnosis and treatment. JAMA 319: 698-710, 2018.
4. Schattauer SS, Bedini A, Summers F, Reilly-Treat A, Andrews MM, Land BB and Chavkin C: Reactive oxygen species (ROS) generation is stimulated by kappa opioid receptor activation through phosphorylated c-Jun N-terminal kinase and inhibited by p38 mitogen-activated protein kinase (MAPK) activation. J Biol Chem 294: 16884-16896, 2019.
5. Negishi T, Matsumoto M, Kobayashi Y, Kojima M, Sakaguchi F, Takahata K, Kanehira T, Arakaki R, Aoyama Y, Yoshida H, *et al*: Dysregulation of MAP kinase signaling pathways including p38MAPK, SAPK/JNK and ERK1/2 in cultured rat cerebellar astrocytes exposed to diphenylarsinic acid. Toxicol Sci 156: 509-519, 2017.
6. Nguyen HT, Hsieh MH, Gaborro A, Tinloy B, Phillips C and Adam RM: JNK/SAPK and p38 SAPK-2 mediate mechanical stretch-induced apoptosis via caspase-3 and -9 in NRK-52E renal epithelial cells. Nephron Exp Nephrol 102: e49-e61, 2006.
7. Chuang HC, Wang X and Tan TH: MAP4K family kinases in immunity and inflammation. Adv Immunol 129: 277-314, 2016.
8. Win S, Than TA and Kaplowitz N: The regulation of JNK signaling pathways in cell death through the interplay with mitochondrial sab and upstream post-translational effects. Int J Mol Sci 19: 3657, 2018.
9. Betigeri S, Pakunlu RI, Wang Y, Khandare JJ and Minko T: JNK1 as a molecular target to limit cellular mortality under hypoxia. Mol Pharm 3: 424-430, 2006.
10. Komatsu W, Kishi H, Yagasaki K and Ohhira S: Urolithin A attenuates pro-inflammatory mediator production by suppressing PI3-K/Akt/NF-kappaB and JNK/AP-1 signaling pathways in lipopolysaccharide-stimulated RAW264 macrophages: Possible involvement of NADPH oxidase-derived reactive oxygen species. Eur J Pharmacol 833: 411-424, 2018.
11. Li B, Zeng M, He W, Huang X, Luo L, Zhang H and Deng DY: Ghrelin protects alveolar macrophages against lipopolysaccharide-induced apoptosis through growth hormone secretagogue receptor 1a-dependent c-Jun N-terminal kinase and Wnt/beta-catenin signaling and suppresses lung inflammation. Endocrinology 156: 203-217, 2015.
12. Zheng Y, Zhang M, Zhao Y, Chen J, Li B and Cai W: JNK inhibitor SP600125 protects against lipopolysaccharide-induced acute lung injury via upregulation of claudin-4. Exp Ther Med 8: 153-158, 2014.
13. Di Conza G and Ho PC: ER stress responses: An emerging modulator for innate immunity. Cells 9: 695, 2020.
14. Amin-Wetzel N, Saunders RA, Kamphuis MJ, Rato C, Preissler S, Harding HP and Ron D: A J-protein Co-chaperone recruits BiP to monomerize IRE1 and repress the unfolded protein response. Cell 171: 1625-1637, 2017.
15. Kopp MC, Larburu N, Durairaj V, Adams CJ and Ali M: UPR proteins IRE1 and PERK switch BiP from chaperone to ER stress sensor. Nat Struct Mol Biol 26: 1053-1062, 2019.
16. Hu R, Chen ZF, Yan J, Li QF, Huang Y, Xu H, Zhang XP and Jiang H: Endoplasmic reticulum stress of neutrophils is required for ischemia/reperfusion-induced acute lung injury. J Immunol 195: 4802-4809, 2015
17. Sommer T and Jarosch E: BiP binding keeps ATF6 at bay. Dev Cell 3: 1-2, 2002.
18. Hsu SK, Chiu CC, Dahms HU, Chou CK, Cheng CM, Chang WT, Cheng KC, Wang HD and Lin IL: Unfolded cprotein response (UPR) in survival, dormancy, immunosuppression, metastasis and treatments of cancer cells. Int J Mol Sci 20: 2518, 2019.
19. Wang M, Law ME, Castellano RK and Law BK: The unfolded protein response as a target for anticancer therapeutics. Crit Rev Oncol Hematol 127: 66-79, 2018.
20. Lee HC and Wei YH: Mitochondrial role in life and death of the cell. J Biomed Sci 7: 2-15, 2000.
21. Estaquier J, Vallette F, Vayssiere JL and Mignotte B: The mitochondrial pathways of apoptosis. Adv Exp Med Biol 942: 157-183, 2012.
22. Xu J, Qin X, Cai X, Yang L, Xing Y, Li J, Zhang L, Tang Y, Liu J, Zhang X and Gao F: Mitochondrial JNK activation triggers autophagy and apoptosis and aggravates myocardial injury following ischemia/reperfusion. Biochim Biophys Acta 1852: 262-270, 2015
23. Wiltshire C, Matsushita M, Tsukada S, Gillespie DA and May GH: A new c-Jun N-terminal kinase (JNK)-interacting protein, Sab (SH3BP5), associates with mitochondria. Biochem J 367: 577-585, 2002.
24. Chambers JW, Pachori A, Howard S, Iqbal S and LoGrasso PV: Inhibition of JNK mitochondrial localization and signaling is protective against ischemia/reperfusion injury in rats. J Biol Chem 288: 4000-4011, 2013.
25. Ngoei KR, Catimel B, Church N, Lio DS, Dogovski C, Perugini MA, Watt PM Cheng HC, Ng DC and Bogoyevitch MA: Characterization of a novel JNK (c-Jun N-terminal kinase) inhibitory peptide. Biochem J 434: 399-413, 2011.
26. Win S, Than TA, Le BH, Garcia-Ruiz C, Fernandez-Checa JC and Kaplowitz N: Sab (Sh3bp5) dependence of JNK mediated inhibition of mitochondrial respiration in palmitic acid induced hepatocyte lipotoxicity. J Hepatol 62: 1367-1374, 2015.
27. Li T, Liu Y, Xu W, Dai X, Liu R, Gao Y, Chen Z and Li Y: Polydatin mediates Parkin-dependent mitophagy and protects against mitochondria-dependent apoptosis in acute respiratory distress syndrome. Lab Invest 99: 819-829, 2019.
28. Win S, Than TA, Fernandez-Checa JC and Kaplowitz N: JNK interaction with Sab mediates ER stress induced inhibition of mitochondrial respiration and cell death. Cell Death Dis 5: e989, 2014.
29. Vannuvel K, Renard P, Raes M and Arnould T: Functional and morphological impact of ER stress on mitochondria. J Cell Physiol 228: 1802-1818, 2013.
30. National Research Council (US): Committee for the Update of the Guide for the Care and Use of Laboratory Animals: Guide for the Care and Use of Laboratory Animals. 8th edition. National Academies Press, Washington, DC, 2011.
31. Chichger H, Rounds S and Harrington EO: Endosomes and autophagy: Regulators of pulmonary endothelial cell homeostasis in health and disease. Antioxid Redox Signal 31: 994-1008, 2019.
32. Glimcher LH, Lee AH and Iwakoshi NN: XBP-1 and the unfolded protein response (UPR). Nat Immunol 21: 963-965, 2020.
33. Li Y, Jiang W, Niu Q, Sun Y, Meng C, Tan L, Song C, Qiu X, Liao Y and Ding C: eIF2alpha-CHOP-BCl-2/JNK and IRE1alpha-XBP1/JNK signaling promote apoptosis and inflammation and support the proliferation of newcastle disease virus. Cell Death Dis 10: 891, 2019.
34. Chambers JW, Cherry L, Laughlin JD, Figuera-Losada M and Lograsso PV: Selective inhibition of mitochondrial JNK signaling achieved using peptide mimicry of the Sab kinase interacting motif-1 (KIM1). ACS Chem Biol 6: 808-818, 2011.
35. Bo L, Li Y, Liu W, Jin F and Li C: Selective inhibition of JNK mitochondrial location is protective against seawater inhalation-induced ALI/ARDS. Mol Med Rep 24: 515, 2021.
36. Win S, Than TA, Han D, Petrovic LM and Kaplowitz N: c-Jun N-terminal kinase (JNK)-dependent acute liver injury from acetaminophen or tumor necrosis factor (TNF) requires mitochondrial Sab protein expression in mice. J Biol Chem 286: 35071-35078, 2011.